FULL TITLE
ASP Conference Series, Vol. **VOLUME**, **YEAR OF PUBLICATION**
NAMES OF EDITORS

Theoretical Developments in Understanding Massive Star Formation

Harold W. Yorke

Jet Propulsion Laboratory, California Institute of Technology, 4800 Oak Grove Drive, Pasadena, CA

Peter Bodenheimer

UCO/Lick Observatory, University of California, Santa Cruz, CA

Abstract. Except under special circumstances massive stars in galactic disks will form through accretion. The gravitational collapse of a molecular cloud core will initially produce one or more low mass quasi-hydrostatic objects of a few Jupiter masses. Through subsequent accretion the masses of these cores grow as they simultaneously evolve toward hydrogen burning central densities and temperatures. We review the evolution of accreting (proto-)stars, including new results calculated with a publicly available stellar evolution code written by the authors. The evolution of accreting stars depends strongly on the accretion history. We find that for the high accretion rates considered $\sim 10^{-3}$ $M_\odot$ yr^{-1}, stars of $\sim$5-10 $M_\odot$ tend to bloat up to radii which may exceed 100 $R_\odot$. Because of the high rate of binarity among massive stars, we expect that these large radii during short phases of evolution will result in mass transfer, common envelope evolution, and a higher number of tight binaries with periods of a few days.

1. Introduction

The collapse of a sufficiently massive molecular clump can produce one or more high mass stars, but – compared to the total number of stars produced – high mass stars are the rare exception and not the rule. Nevertheless, when one or more high mass stars form, they dominate the evolution of the parent molecular cloud and control subsequent star formation through their winds, ionizing radiation and, ultimately, supernova explosions. In spite of their importance to the star formation process in general, to the production of heavy elements and to the overall evolution of galaxies, our understanding of high mass star formation is still rather sketchy. The process of forming a massive star is not a straightforward scaled-up version of low mass star formation.

Several theoretical aspects of massive star formation are addressed in recent reviews. To mention a few: *Toward Understanding Massive Star Formation* (Zinnecker & Yorke 2007), *Theory of Star Formation* (McKee & Ostriker 2007), *The Formation of Massive Stars* (Beuther et al. 2007), and *Disks Around Young O-B (Proto-)Stars: Observations and Theory* (Cesaroni et al. 2007), and *Clustered Massive Star Formation in Molecular Clouds* (Tan 2005). One theoretical aspect of massive star formation only briefly mentioned in the first-cited review but not discussed in the others is the expected evolution of accreting (proto-) stars.

Massive stars seldom form individually; multiple systems, clusters and associations are the general rule. Outflows, pressure and radiative effects from multiple sources will strongly influence but not prevent the formation of massive stars via accretion. Accretion growth of an initially low mass object up to high masses will occur through a circumstellar disk. This requires high accretion rates onto the disk and through the disk onto the central star, in excess of 10^{-4} $M_\odot$ yr^{-1}. Accretion onto the embryo massive star is likely to be highly variable. Central hydrogen burning begins while the young massive star continues to accrete material, and it simultaneously photoevaporates its circumstellar disk and nearby disks on a timescale of $\sim 10^5$ yr. The final mass of the central star and nearby neighboring systems is determined by the interplay between radiation acceleration, UV photoevaporation, stellar winds and outflows, and details of the accretion process.

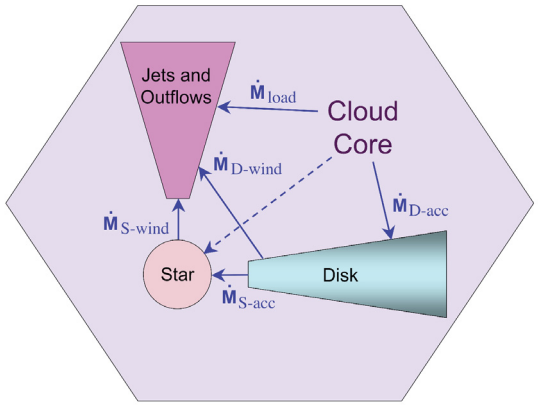

Figure 1. A schematic view of accretion and mass loss. Only a fraction of the material accreted onto the disk will settle onto the star. The measured outflows will have contributions from the star, its disk, and swept up molecular material.

In the following we concentrate on the evolution of the accreting object.

2. A Simple Model for Accreting Stars

We can expect that an accreting star has a significantly different evolution than a non-accreting star. Some of the main differences can be derived from simple theoretical arguments.

2.1. Basic equations

Following Yorke & Sonnhalter (2002) we can express the total energy of a hydrostatic object in terms of a "structure parameter" η:

$$E_{\rm tot} = -\eta \frac{GM^2}{R} \ , \qquad (1)$$

where M and R are the mass and radius of the object and η is a parameter which describes its compactness. For polytropes of degree n, $\eta = 3/(10-2n)$ (e.g. Kippenhahn & Weigert 1990). Thus, for a fully convective pre-main sequence protostar ($n = 3/2$) $\eta = 3/7$. As the star approaches the main sequence, a greater proportion of it becomes radiative, its core becomes more compact, and η increases.

Assuming hydrostatic and thermal equilibrium and a constant chemical composition, existing stellar models of non-accreting stars can be used to approximate $\eta = \eta(M, R)$ as a function of known parameters. The intrinsic core luminosity L (which excludes the contribution to the total luminosity emitted outside the star as material falls from infinity to the radius R) is given by:

$$\begin{aligned} L &= L_{\rm nuc} - \dot{E}_{\rm tot} - \beta\frac{GM\dot{M}}{R} \\ &= L_{\rm nuc} - E_{\rm tot}\left[\frac{\dot{\eta}}{\eta} + \left(2 - \frac{\beta}{\eta}\right)\frac{\dot{M}}{M} - \frac{\dot{R}}{R}\right] \end{aligned} \tag{2}$$

where $L_{\rm nuc}$ is the contribution from nuclear burning, $\dot{M}$ is the accretion rate of material infalling onto the star, and $L_{\rm acc} = \beta GM\dot{M}/R$ is the accretion luminosity ($\beta \approx 1$). When discussing the total bolometric luminosity of a spherically accreting star, however, one has to include the contribution of the potential energy of infalling material dissipated on its way to the stellar surface: $L_{\rm bol} = L + L_{\rm acc} = L_{\rm nuc} - \dot{E}$.

For the pre-main sequence phase we shall account for deuterium burning only and use the following approximate expression:

$$L_{\rm nuc} = L_D \approx L_0(M)\left[\frac{\chi_D}{\chi_{D,0}}\right]\left[\frac{R_0(M)}{R}\right]^p , \tag{3}$$

where L_0 and R_0 are the equilibrium deuterium burning rate and equilibrium radius for a star of mass M at its "birthline", $\chi_{D,0}$ is the cosmic mass abundance of deuterium, and χ_D is the star's net deuterium abundance. We have chosen $p = 21$ to insure that a non-accreting star remains close to its birthline until a significant fraction of its deuterium is consumed. Assuming instantaneous mixing during accretion, the deuterium mass fraction χ_D can be calculated:

$$\frac{d\chi_D M}{dt} = \chi_{D,0}\dot{M} - \epsilon_D L_D , \tag{4}$$

where $\epsilon_D L_D$ is the rate of deuterium consumption due to deuterium burning and $\epsilon_D = 1.76 \times 10^{-19}\,{\rm s}^2\,{\rm cm}^{-2}$ is a constant.

From equation 2 we can derive an expression for $\dot{R}$:

$$\frac{\dot{R}}{R} = \frac{1}{1-\eta_R}\left(\left[2 - \frac{\beta}{\eta} + \eta_M\right]\frac{\dot{M}}{M} + \frac{L - L_{\rm nuc}}{E_{\rm tot}}\right) \tag{5}$$

where $\eta_R = (\partial \ln\eta/\partial \ln R)_M$ and $\eta_M = (\partial \ln\eta/\partial \ln M)_R$. We used a grid of pre-main sequence models calculated with the stellar evolution code described by Bodenheimer et al. (2007) to tabulate $\eta(M,R)$, $L(M,R)$, $L_0(M)$, and $R_0(M)$ (see Fig. 2). We then approximate the pre-main sequence evolution of an accreting protostar by integrating equations 4 and 5 simultaneously.

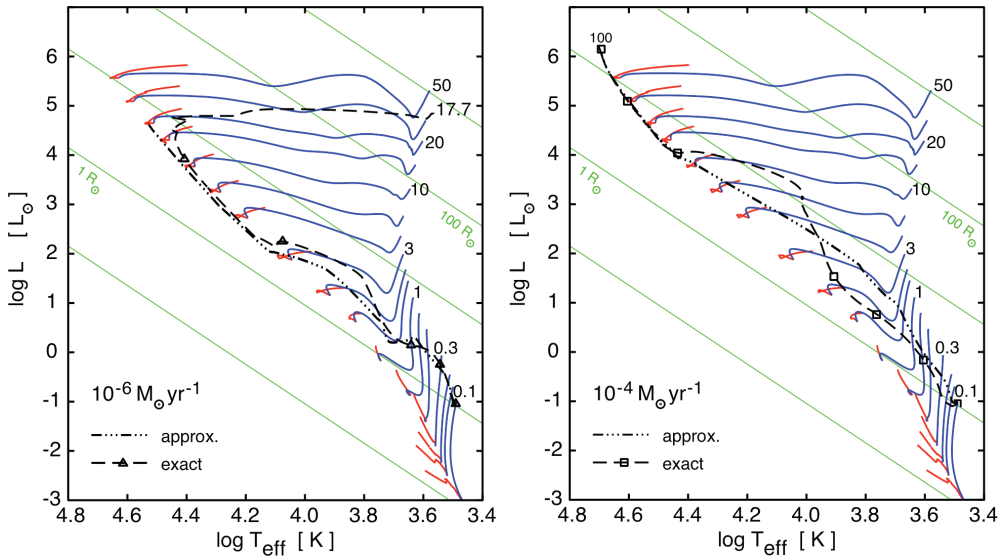

Figure 2. Evolutionary tracks of accreting stars in the Hertzsprung-Russell diagram using an approximate model for stellar evolution (dashed-dotted lines) described in section 2.1., and using the stellar evolution code (dashed lines) described in section 3.. Symbols (triangles and squares) denote the positions for $M(t)/\mathrm{M}_\odot = 0.1$, 0.3, 1, 3, 10, and 30. Pre-main-sequence and main-sequence tracks of non-accreting stars for masses $M/\mathrm{M}_\odot = 0.1$, 0.15, 0.2, 0.3, 0.5, 0.7, 1, 1.5, 2, 3, 5, 7, 10, 15, 20, 30, 50 are shown (solid lines) for comparison.

2.2. Results of simplified model

We display in Fig. 2 the evolution of accreting stars using the simplified model described above and assuming constant accretion rates as indicated. These tracks are compared with those calculated with a full stellar evolution code, described in section 3. below. The initial condition is a protostellar core of 0.1 $\mathrm{M}_\odot$ and a radius of about 1 $\mathrm{R}_\odot$, giving a central temperature of 8×10^5 K. The composition is solar with an initial deuterium mass fraction of 4×10^{-5}. The mass at which the accreting protostar reaches the main sequence, defined as the point of minimum radius at the onset of hydrogen burning, is 3.3 $\mathrm{M}_\odot$ for the accretion rate of 10^{-6} $\mathrm{M}_\odot$ yr^{-1} and 10 $\mathrm{M}_\odot$ for the accretion rate of 10^{-4} $\mathrm{M}_\odot$ yr^{-1}. The arrival at the main sequence is determined by the point where the accretion time scale $M/\dot{M}$ is longer than the pre-main-sequence contraction time (2×10^6 yr for 3 $\mathrm{M}_\odot$ and 10^5 yr for 10 $\mathrm{M}_\odot$). The results of the more precise calculations are discussed in further detail in Section 4..

Differences between the results of the simplified model and the more detailed stellar evolution calculations can be attributed to the assumption of thermal equilibrium for the simplified model. This assumption is justified for accretion rates $\sim 10^{-6}$ $\mathrm{M}_\odot$ yr^{-1}, but not for higher accretion rates. Nevertheless, for both of our comparison cases depicted in Fig. 2 the arrival times and masses at the main sequence predicted by the simplified model are reasonably correct.

3. Evolution of Accreting (Proto-)Stars

The evolution of accreting stars have been calculated by several authors. Kippenhahn & Meyer-Hofmeister (1977) considered accretion of mass onto the main-sequence secondary in a binary system with Roche-lobe overflow from the primary. The primary is not included and the accretion rate is taken to be a constant. Although not strictly applicable to the case of high mass star formation, these calculations show how the evolution of stars is modified when accretion occurs. Even in the case of high mass star formation, it is conceivable that accretion flares up again after a star has settled onto the main sequence. The authors assumed various starting masses and accretion rates and thus provide test cases for newer codes. An important result of these studies is the rapid increase of radius when main sequence stars of a few solar masses accreted material at high accretion rates (10^{-4} $M_\odot$ yr^{-1} and higher).

Palla & Stahler (1992) considered the evolution of intermediate mass protostars (2-10 $M_\odot$) with constant accretion rates 10^{-5}, 3×10^{-5}, and 10^{-4} $M_\odot$ yr^{-1}. Their highest accretion rate provides a comparison case for our code (see below) and can be considered as the lower end of the appropriate accretion rates for high mass star formation.

Norberg & Maeder (2000), Behrend & Maeder (2001), Yorke (2002), and Hosokawa (this conference) have all considered the evolution of accreting protostars under a variety of conditions. Yorke (2002) used the simplified model discussed in section 2.1. with earlier non-accreting tracks and found similar behavior to that shown in Fig. 2. Norberg & Maeder (2000) and Behrend & Maeder (2001) assumed variable accretion rates which increased as the stellar mass grew. The accretion rates were too low when the stars were in the 3-10 $M_\odot$ range and the masses were too high when the accretion rates were high, so that no significant "bloating" (rapid increase of radius) was noted. Hosokawa and the present authors presented results showing that bloating occurs in the intermediate mass range if the accretion rate is sufficiently high.

3.1. The detailed model

Using a full stellar evolution computer code, we have calculated a parallel sequence of accreting stars. The code solves the standard four differential equations of stellar structure in spherical symmetry using the Henyey method. The model stars are divided into two regions, the interior, which includes most of the mass, and the atmosphere, which provides the surface boundary condition through a detailed inward integration of the equations of hydrostatic equilibrium and radiative or convective transfer. The atmosphere is integrated inward with a Runge-Kutta procedure to a layer with a temperature that varies with time, but is typically $\sim 10^5$ K. Mass is added at a given fixed rate and is deposited in the atmosphere at the same temperature and density as the material in that region. By means of an automatic rezoning procedure, the added material is incorporated into the stellar interior. The composition of the added material is the same as that of the initial star and includes deuterium in approximately the cosmic abundance. Mass zones are added or subtracted from the interior to optimize accuracy.

The physics in both the interior and atmosphere includes:

- mixing-length theory in convection zones, whereby $\lambda_{\rm MLT} = 2$

- a detailed equation of state, including electron degeneracy, radiation pressure, and non-ideal effects from the tables of Saumon et al. (1995)
- interior Rosseland mean opacities from the publically available OPAL tables (Iglesias & Rogers 1996) and low-temperature opacities, including molecular contributions, from Alexander & Ferguson (1994)
- nuclear burning of deuterium as well as non-equilibrium burning of hydrogen by the proton-proton cycle and the CNO cycle. Nuclear parameters are primarily from Bahcall (1989).

Further details on the code are provided in the book by Bodenheimer et al. (2007).

3.2. Testing the detailed model

Two test calculations have been performed, including the effects of accretion, to show that the code produces reasonable results. Palla & Stahler (1992) computed the evolution of accreting protostars using a simple photospheric boundary condition

$$\kappa P = \frac{2}{3} g \qquad \text{and} \qquad L = 4\pi R^2 \sigma T_{\rm eff}^4 \tag{6}$$

where g is the surface acceleration of gravity, P and κ are, respectively, the photospheric pressure and Rosseland mean opacity, $T_{\rm eff}$ is the photospheric temperature, and L, R, are respectively, the total luminosity and radius. Although we use a model atmosphere to provide a similar outer boundary condition, the basic assumption is the same, namely that only the internal luminosity generated by nuclear burning and contraction is included in L. The accretion luminosity $L_{\rm acc}$ is assumed to be radiated away outside the young star. In addition, we do not modify L for effects of reddening or extinction caused by circumstellar material.

Our comparison with Palla & Stahler (1992) is done with an accretion rate of 10^{-4} $M_\odot$ yr^{-1} and an initial deuterium abundance of $D/H = 2.5 \times 10^{-5}$ by number. The initial condition was similar but not identical to theirs: a star of 1.3 $M_\odot$ at a radius of about 4 $R_\odot$ and a central temperature of 2.3×10^6 K with a fully convective structure. Figure 3 shows the subsequent behavior of luminosity and radius as a function of M. In our case, at a mass of 4.5 $M_\odot$ there is a sudden rapid increase in radius. A maximum radius of 15 $R_\odot$ is reached, close to the maximum of 16 $R_\odot$ obtained by Palla & Stahler (1992) at a slightly higher mass. The increase is generated when the star becomes fully radiative, although the central temperature is not yet high enough to support hydrogen burning. The deuterium in the deep interior has been completely burned, but the deuterium that is added at each time step burns in a shell at temperatures between 1.5 and 2 $\times 10^6$ K. Once the star has thermally adjusted to this shell source the radius begins to decrease and internal temperatures increase. Our sequence was carried to 12.5 $M_\odot$ at which point the star is approaching the hydogen-burning main sequence with a convective core, and the thermal adjustment time scale is shorter than the mass accretion time scale. The agreement with Palla & Stahler (1992) is satisfactory, considering the differences in initial conditions and physics.

The second test calculation was a comparison with Kippenhahn & Meyer-Hofmeister (1977). The comparison case we pick is a main sequence star of 5 $M_\odot$ accreting deuterium-free material at a rate of 10^{-3} $M_\odot$ yr^{-1}. In the initial model, the time scale of accretion is far shorter than the thermal adjustment time

scale, so the star must expand to accommodate the added mass. The expansion is rapid and is accompanied by an increase in luminosity, so eventually the point is reached where the thermal adjustment time becomes shorter than the accretion time. Then a slow contraction occurs, along with a continued increase in L. Kippenhahn & Meyer-Hofmeister (1977) obtain a maximum radius of 4×10^{12} cm at a mass of 9 $M_\odot$, while we get 8×10^{12} cm at 10 $M_\odot$. Note that our opacities are considerably different from the older ones they use. The main sequence is not reached until $M \approx 27$ $M_\odot$, also in reasonable agreement with their results.

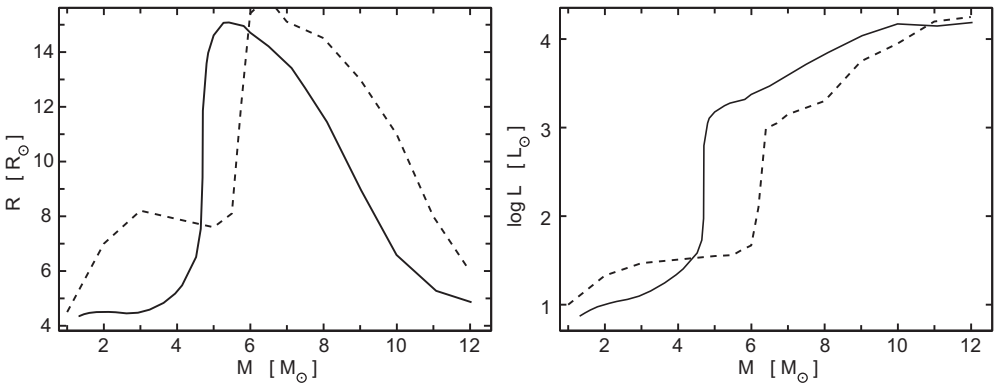

Figure 3. Radius (left) and luminosity (right) as a function of mass for accreting protostars with an accretion rate of 10^{-4} $M_\odot$ yr^{-1}, as calculated by the present authors (*solid*) and by Palla & Stahler (1992) (*dashed*).

4. Results and Discussion

In addition to the evolution of accreting protostars at rates 10^{-6} $M_\odot$ yr^{-1} and 10^{-4} $M_\odot$ yr^{-1} shown in Fig. 2 we have performed calculations for accretion rates of 10^{-3} $M_\odot$ yr^{-1} and 10^{-2} $M_\odot$ yr^{-1} (see Fig. 4). Note that in order to produce a 20 $M_\odot$ (100 $M_\odot$) star within 2×10^5 yr (10^5 yr) an average accretion rate 10^{-4} $M_\odot$ yr^{-1} (10^{-3} $M_\odot$ yr^{-1}) is necessary, but if accretion is highly variable, even higher instantaneous accretion rates must occur. For each case the initial condition is a protostellar core of 0.1 $M_\odot$ and a radius of about 1 $R_\odot$ with solar composition and a deuterium mass fraction of 4×10^{-5}.

For the accretion rate of 10^{-6} $M_\odot$ yr^{-1} the evolution can be divided into a pre-main-sequence phase for mass less than 3.5 $M_\odot$, a main-sequence phase up to a mass 16.6 $M_\odot$, and a post-main-sequence phase above that mass. During the pre-main-sequence evolution the results of the detailed calculation are similar to those found in the simple model – accretion time scales are short compared with contraction times to the main sequence, so the evolutionary track crosses the constant-mass tracks, staying mostly convective until 1.5 $M_\odot$ is reached. The deuterium-burning luminosity induced by the infall of fresh deuterium is only 1.5 $L_\odot$ at this accretion rate, thus beyond 1.5 $M_\odot$ it is not significant. Once the main sequence is reached, the accretion time scale is longer than the thermal

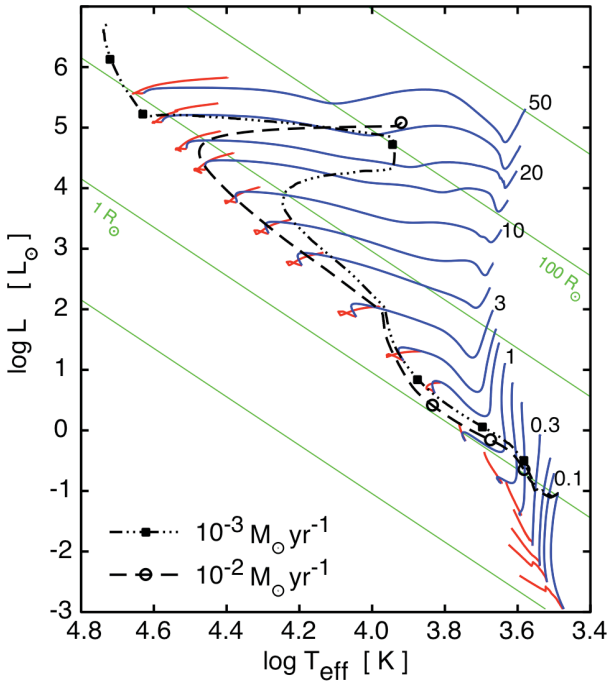

Figure 4. Evolution of accreting stars with different constant accretion rates as indicated were calculated using the stellar evolution code supplied with the book by Bodenheimer et al. (2007). Non-accreting pre-main-sequence tracks (blue lines) and main sequence tracks (red lines) are displayed for masses denoted at the beginning of the tracks. Symbols (filled squares and open circles) denote the positions after 0.3, 1, 3, 10, 30, and 100 $M_\odot$ have been accreted.

adjustment time, and the star simply moves up the main sequence. The total time needed to accrete to 17 $M_\odot$, 1.7×10^7 yr, is longer than the main sequence lifetime at that mass, so at a slightly lower mass the evolutionary track heads toward the red giant region.

At 10^{-4} $M_\odot$ yr^{-1} the evolution differs significantly from that predicted by the simple model. The main deviation occurs because of the departure from thermal equilibrium induced by the burning of the accreted deuterium in a thin shell, as described above in the comparison with Palla & Stahler (1992). The details are different because of the different initial condition, but the main effect is there – the expansion of the star to 15 $R_\odot$ once it becomes fully radiative at a mass of about 5 $M_\odot$. The main sequence is reached at about 10.8 $M_\odot$, and the remainder of the evolution simply follows the main sequence to higher masses, as the accretion time scale is shorter than the main-sequence lifetime but longer than the thermal adjustment time. We show results up to 100 $M_\odot$ ($t_{\rm evol} = 10^6$ yr).

At 10^{-3} $M_\odot$ yr^{-1} (Fig. 4) at low masses the accretion time scale is far shorter than the contraction time as well as the thermal adjustment time, so the object does not reach thermal adjustment until the mass grows to about 10 $M_\odot$.

The initial configuration is fully convective, and it remains so until just above 1 $M_\odot$. At 0.5 $M_\odot$ the interior luminosity reaches about 500 $L_\odot$ from deuterium burning, but the radiative surface boundary allows only 1 $L_\odot$ to escape. The added deuterium burns immediately, and the equilibrium deuterium abundance, uniform through the convective star, is about 10^{-7} by mass. As shown by the track, the radius, after a slight initial expansion, remains nearly constant at just under 2 $R_\odot$ during the fully convective phase. Above 1 $M_\odot$ the radiative core grows in mass, but the deuterium still burns and mixes in a deep convective envelope. At 3 $M_\odot$ the convection zone includes about 10% of the stellar mass and extends down to a temperature of 3.8×10^6 K, so the deuterium is still able to burn and mix in the convection zone. At 5 $M_\odot$ the star becomes fully radiative ($T_{\rm eff} = 10,600$ K) and deuterium shell burning sets in. A maximum luminosity of 2000 $L_\odot$ is produced in the interior, but only 300 $L_\odot$ is radiated at the surface. This departure from thermal equilibrium is accompanied by a rapid expansion and an increase in luminosity to 10^4 $L_\odot$ in 200 yr. A maximum in $T_{\rm eff}$ at 17,000 K is reached with the mass still slightly above 5.1 $M_\odot$. The expansion and brightening then continue at a slower pace until a maximum radius of 100 $R_\odot$ is reached at a mass of 10 $M_\odot$. At this point there is a small central convection zone as a result of the initial conversion of carbon to nitrogen in the CNO cycle, but the outer regions remain radiative.

The final phase, in which accretion time and thermal adjustment time are closely matched, involves a decrease in radius and slow increase in luminosity, until the main sequence is reached at 28.5 $M_\odot$ with a radius of 7.46 $R_\odot$ and a luminosity of 1.5×10^5 $L_\odot$. The sequence is calculated up to 200 $M_\odot$ ($t_{\rm evol} = 2 \times 10^5$ yr), at which point the central hydrogen has been depleted to a mass fraction of 0.67, compared to the initial value of 0.71. Thus the accretion time scale is still shorter than the main-sequence nuclear time scale.

Many general aspects of the evolution with accretion rates in excess of 10^{-4} $M_\odot$ yr^{-1} were also found for the calculation assuming an accretion rate 10^{-2} $M_\odot$ yr^{-1} (Fig. 4). Early in the evolution at low masses the accretion time scale is far shorter than the time scales for contraction and thermal adjustment. Positions in the Herzsprung-Russell diagram for 0.3, 1, 3, and 10 $M_\odot$ do not fall on the corresponding evolutionary tracks of non-accreting stars – violating a key assumption made for the simplified model discussed in section 2.1.. Initially fully convective, about 60% of the stellar mass is radiative after 1.6 $M_\odot$ have accreted. At this point the stellar radius and luminosity are 1.2 $R_\odot$ and 1 $L_\odot$, respectively, although internally about 350 $L_\odot$ from deuterium burning is produced. After 9 $M_\odot$ have accumulated ($t_{\rm evol} = 900$ yr) the stellar luminosity has climbed to 100 $L_\odot$, although in excess of 10^5 $L_\odot$ are produced internally by deuterium shell burning and central CNO-cycle hydrogen burning. The star is not in thermal equilibrium. The evolutionary track has just intersected the non-accreting track for a 3 $M_\odot$ star. 20 yr later the stellar luminosity has jumped by a factor of almost 300 to 2.7×10^4 $L_\odot$ with an effective surface temperature 28,700 K and only a modest increase of radius. Central CNO-burning is the principle source of energy production and the inner 3.7 $M_\odot$ core is convective. Over the course of the next 70 yr the star expands to over 180 $R_\odot$ with a stellar luminosity of 1.4×10^5 $L_\odot$. At this point we stopped the calculations; the star had grown to 10 $M_\odot$.

The calculation with an accretion rate of 10^{-3} $M_\odot$ yr^{-1} was repeated without deuterium in the accreted material. Whereas the star accreting material with deuterium was radiative everywhere except in atmospheric convection zones after 5 $M_\odot$ had been accreted, the deuterium-free accreting star remained fully convective up to a mass 10 $M_\odot$. Between 12 $M_\odot$ and 15 $M_\odot$ there was a CNO-cycle hydrogen burning convective core of 9.3 $M_\odot$. The outer convection zone shrank from 2% to 0.03% of the stellar mass. However, in spite of the high accretion rate, no rapid expansion took place because of the short thermal adjustment time at that mass. After an initial contraction to about 0.37 $R_\odot$ at 1.2 $M_\odot$, the radius gradually increased to a maximum of 7 $R_\odot$ at 23 $M_\odot$.

The discriminator as to whether or not an accreting star expands to several tens of $R_\odot$ or even to greater than 100 $R_\odot$ is not whether or not the accreting material contains deuterium. The comparison to the Kippenhahn & Meyer-Hofmeister (1977) calculations assumed accretion of deuterium-free material onto a main sequence 5 $M_\odot$ star at a rate 10^{-3} $M_\odot$ yr^{-1}. By the time the stellar mass had grown to 10.2 $M_\odot$, it had expanded to 115 $R_\odot$. The discriminator as to whether or not an accreting star bloats up is whether or not the star is radiative and in the mass range ∼3-10 $M_\odot$ when accretion occurs at a high rate. Our current grid of models is too coarse to restrict precisely the mass range and range of accretion rates which induce bloating. This will be the subject of a more detailed investigation (Yorke & Bodenheimer, in prep.).

5. Conclusions and Outlook

Because of the high rate of binarity among O-stars and preponderance of tight binaries with periods of the order of days (see discussion by Zinnecker & Yorke 2007), the concept of bloating during the accretion phase is an important aspect of high mass star formation. An expansion to radii of ∼100 $R_\odot$ greatly increases the cross section for stellar collisions and near collisions. Mass transfer between sufficiently close binaries can occur – in extreme cases resulting in a common envelope of the binaries. During episodes of common envelope evolution even tighter binaries can be formed or coalescence of the binaries may result. Finally, the accretion process itself from the disk onto the star can be strongly enhanced by the sudden radius growth of the star as the inner parts of the disk are enveloped.

Acknowledgments. Part of this work was performed at the Jet Propulsion Laboratory, operated by the California Institute of Technology under contract to the National Aeronautics and Space Administration (NASA). HWY is partially supported by NASA under the auspices of the "Origins of Solar Systems" Program and grant 05-SSO05-20.

References

Alexander, D., Ferguson, J., 1994, *ApJ*, 437, 879
Bahcall, J. N., 1989, *Neutrino Astrophysics* (Cambridge: Cambridge Univ. Press)
Behrend, R., Maeder, A., 2001, *Astron. Astrophys.*, 373, 190

Beuther, H., Churchwell, E.B., McKee, C. F., Tan, J. C., 2007, in *Protostars and Planets V*, eds. B. Reipurth, D. Jewitt, and K. Keil, (Tucson: University of Arizona Press), p.165

Bodenheimer, P., Laughlin, G. P., Rozyczka, M., Yorke, H. W., 2007, *Numerical Methods in Astrophysics: An Introduction*, (New York: Taylor & Francis)

Cesaroni, R., Galli, D., Lodato, G., Walmsley, C. M., Zhang, Q., 2007, in *Protostars and Planets V*, eds. B. Reipurth, D. Jewitt, and K. Keil, (Tucson: University of Arizona Press), p.197

Iglesias, C., Rogers, F., 1996, *ApJ*, 464, 943

Kippenhahn, R., Meyer-Hofmeister, E., 1977, *Astron. Astrophys.*, 54, 539

Kippenhahn, R., Weigert, A., 1990, *Stellar Structure and Evolution*, (Berlin: Springer)

McKee, C. F., Ostriker, E. C., 2007, *Ann. Rev. Astron. Astrophys.*, 45, 565

Norberg P., Maeder A., 2000, *Astron. Astrophys.*, 359, 1025

Palla, F., Stahler, S. W., 1992, *ApJ*, 392, 667

Saumon, D., Chabrier, G., van Horn, H., 1995, *ApJ Suppl*, 99, 713

Tan, J. C., 2005, in Proceedings IAU Symposium 227, eds. R. Cesaroni, E. Churchwell, M. Felli, C. M. Walmsley, p. 318

Yorke, H. W., Sonnhalter, C., 2002, *ApJ*, 569, 846

Yorke, H. W., 2002, in *Hot Star Workshop III: The Earliest Stages of Massive Star Birth*. ASP Conference Proceedings, Vol. 267, ed. P. A. Crowther, p.165

Zinnecker, H., Yorke, H. W., 2007, *Ann. Rev. Astron. Astrophys.*, 45, 481